Pharm Res (2016) 33:2358–2372
DOI 10.1007/s11095-016-1944-y

EXPERT REVIEW

# Polymer-Based and pH-Sensitive Nanobiosensors for Imaging and Therapy of Acidic Pathological Areas

Yi Li[1] • Hong Yu Yang[1] • Doo Sung Lee[1]

Received: 10 March 2016 / Accepted: 11 May 2016 / Published online: 16 May 2016


**ABSTRACT** Nanobiosensors with high sensitivity and specificity have shown great potential in the detection of diseases. The incorporation of therapeutic agents with nanobiosensors allows the simultaneous diagnosis and therapy of diseases. The delivery of nanobiosensors and therapeutic agents using polymers is a common strategy to improve imaging and therapeutic efficacies. These polymers play important roles in several aspects during a successful delivery process, such as increasing the stability and biocompatibility of the nanobiosensors and improving their cell endocytosis. The pH-sensitivity of the nanobiosensors endows them with various capabilities, such as enabling the selective targeting of pathological areas, activation of imaging signals and controlled release of payloads. This review focuses on the design, preparation and characterization of polymer-based and pH-sensitive nanobiosensors and the *in intro*/*in vivo* assessment of their ability to serve as efficient agents for the diagnosis and therapy of acidic pathological areas.

**KEY WORDS** biocompatible polymers · bioimaging · pH-sensitive nanobiosensor · systemic delivery · theranostics

✉ Doo Sung Lee
dslee@skku.edu

[1] Theranostic Macromolecules Research Center, School of Chemical Engineering, Sungkyunkwan University, Suwon, Gyeonggi-do 16419 South Korea

## ABBREVIATIONS

| | |
|---|---|
| DOTA | 1,4,7,10-tetraazacyclododecane-1,4,7, 10-tetraacetic acid |
| DOX | Doxorubicin |
| EPR | Enhanced permeability and retention |
| LCST | Lower critical solution temperature |
| MR | Magnetic resonance |
| NBD | 4-(2-methylacryloyloxyethylamino)-7-nitro-2,1, 3-benzoxadiazole |
| PAA | Poly(acrylic acid) |
| PAE | Poly(β-amino ester) |
| PDPA | Poly[2-(diisopropylamino)ethyl methacrylate] |
| PEG | Poly(ethylene glycol) |
| PNIPAm | Poly(N-isopropylacrylamide) |
| PpIX | Protoporphyrin IX |
| SPIONPs | Superparamagnetic iron oxide nanoparticles |
| TMR | Tetramethylrhodamine |
| TRITC | Tetramethylrhodamine iso-thiocyanate |

## INTRODUCTION

During the last two decades, polymer-based nanobiosensors have been widely studied and applied for detecting pathological areas (1). In general, polymer-based nanobiosensors can be fabricated by physically encapsulating or chemically conjugating imaging agents (such as inorganic nanoparticles or fluorescent dyes) to polymeric nanoparticles with various morphologies. In these types of nano systems, polymers play an important role in improving the aqueous stability of imaging agents, efficiently delivering imaging agents to pathological areas, and enhancing the imaging. By using different imaging methods, polymer-based nanobiosensors have shown unique advantages and great potential in the diagnostics and monitoring of pathological areas. These methods include magnetic

resonance imaging, optical imaging, ultrasonography, positron emission tomography, and X-ray computed tomography (2,3). Sometimes, these methods are combined to more accurately detect pathological changes.

Currently, polymer-based nanobiosensors are mostly used to detect cancers. Cancer is a leading cause of patient death all over the world but is difficult to detect and cure. Nanobiosensors are advantageous in detecting cancer due to a phenomenon called the "EPR effect" (Fig. 1), which has been demonstrated to be universal in solid tumors (4–11). It has been proved that vascular permeability is significantly higher in tumors than in normal organs or tissues. This phenomenon allows nanoparticles with an appropriate size (generally between 10 nm and 200 nm) to be passively accumulated at tumor sites during circulation in the bloodstream, and the concentration of nanoparticles in tumor tissues could be 10–200 times higher than that in normal tissues. Polymer-based nanobiosensors are also employed to detect stroke and other diseases (12–14). To detect and cure diseases at the same time, therapeutic agents are incorporated into traditional nanobiosensors (15). These nanobiosensors with both diagnostic and therapeutic abilities are sometimes called "nano theranostic agents".

Owing to their good biocompatibility and unique physical and chemical properties, polymers are frequently used by scientists in the construction of nanobiosensors. These polymers can be classified into two categories: synthetic (such as polyesters, polypeptides, or polycarbonates) and natural (such as chitosan, dextran, or starch). In different design concepts of polymer-based nanobiosensors, the functions of the polymers are also different. For example, PEG is the most frequently used polymer for this purpose and has been proven to be effective in the enhancement of tumor targeting due to the elongation of the circulation time of the nanobiosensors in the bloodstream. Polymers are also used to encapsulate hydrophobic imaging and therapeutic agents, target specific pathological areas, and enhance imaging of pathological areas.

Compared with conventional polymers, stimulus-sensitive polymers are more important and are extensively employed to more effectively detect pathological areas. Stimulus-sensitive polymers are normally responsive to small external or internal environment changes, which results in a structural change and a subsequent property change of the polymers. Under this concept, pH-sensitive polymers (14,16), temperature-sensitive polymers (17–19), redox-sensitive polymers (20), light-sensitive polymers (21) and many other intelligent polymers have been incorporated with imaging agents to prepare nanobiosensors. Among these stimuli, the pH change is the most important because of the acidity of many solid tumors, caused by their higher rate of lactic acid production compared with normal cells (22). The extracellular pH values of cancer tissues range from 6.0 to 7.0, which is lower than the pH value of normal tissues (pH 7.4) (23–27). The pH values of the endosomes of tumor cells are even lower, ranging from 4.5 to 5.5; this pH difference allows nanoparticles with appropriate pH sensitivity to release their payloads inside tumor cells (26,28). The acidic nature of the tumor extracellular and intracellular environments provides an opportunity to design pH-sensitive nanobiosensors that are more powerful in tumor imaging. It should be noted that acidity is a universal phenomenon in solid tumors (29). The pH value may vary from tumor to tumor, but it is always lower than that of normal tissues (29,30).

In this review, we will summarize important advances (mostly published within the last 5 years) in the field of the imaging and therapy of diseases using polymer-based pH-sensitive nanobiosensors. We mainly focus on the design of polymer-based and pH-sensitive nanobiosensors and their

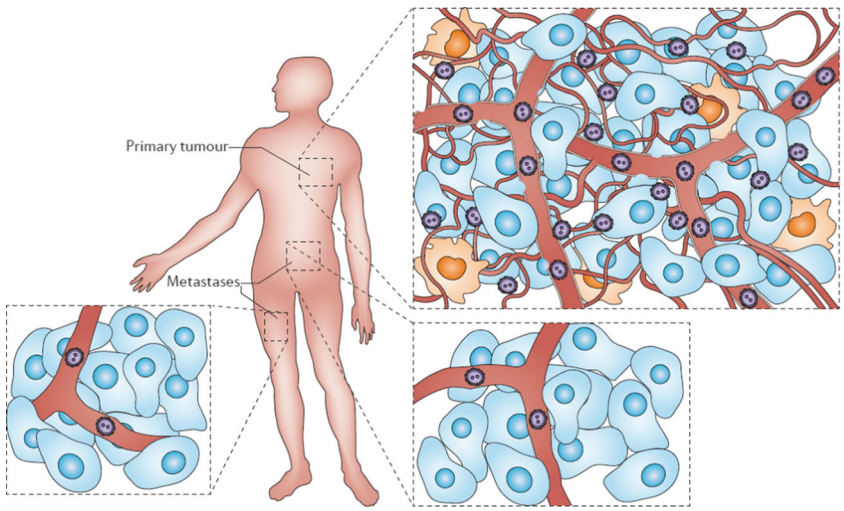


**Fig. 1** Illustration of the EPR effect. The EPR effect allows nanoparticles to be passively accumulated at the tumor site due to porous structure of tumor blood vessels. However, nanoparticles cannot accumulate at small metastases due to poorly vascularized structure of their blood vessels. Reproduced with permission (4).

*in vitro* and *in vivo* assessment. At the end of this review, we will highlight the remaining problems and trends in this research field.

## POLYMER-BASED AND PH-SENSITIVE NANOBIOSENSORS

Polymer-based pH-sensitive nanobiosensors could be prepared from ionizable-group or acid-labile group-containing pH-sensitive polymers that are physically or chemically incorporated with imaging agents. Under acidic conditions, these pH-sensitive polymers could change from hydrophobic to hydrophilic, resulting in the disassociation of the nanostructures of nanobiosensors and leading to the release of imaging agents or the activation of imaging signals (14,16). Polymer-based pH-sensitive nanobiosensors could also be prepared from non-pH-sensitive polymers that are chemically linked with imaging agents or drugs through acid labile bonds.

Because the pH differences between normal tissues and pathological tissues are very small, only chemical groups that are responsive to slight pH changes can be utilized to prepare pH-sensitive nanobiosensors for the diagnosis of disease. The ionization of the tertiary amine groups of polymers generally makes the polymers change from hydrophobic to hydrophilic and then breaks down the polymeric nanostructures, so many researchers have tried to control the pKa of the amine groups of polymers and employ those polymers for sensing small pH changes for imaging and therapy applications (31). Acid-labile bonds that can be cleaved under mildly acidic conditions are also good candidates for designing pH-sensitive nanobiosensors. Hydrazone, acetal and benzoic amine bonds are the most popular candidates because of their responsiveness to slight pH changes (32).

### Polymer-based and PH-Sensitive Nanobiosensors for MR Imaging

For many years, SPIONPs have been used as the most important contrast agents for MR imaging because of their unique magnetic properties with strong shortening effects under longitudinal relaxation ($T_1$) and transverse relaxation ($T_2$) (33). The encapsulation of SPIONPs into pH-sensitive polymeric nanoparticles could remarkably enhance their accumulation at pathological areas and thus provide improved imaging of those areas. Our group has conducted some pioneering work in the delivery of SPIONPs using a pH-sensitive amphiphilic polymer (PEG-*block*-PAE) bearing ionizable tertiary amine groups for the diagnosis of brain ischemia (12). Due to the accumulation of lactic acid produced by anaerobic glycolysis, the pH of ischemic tissues is lower than that of normal tissues. With this concept, we designed a pH-sensitive amphiphilic polymer that can self-assemble into nanoparticles in aqueous solutions at pH 7.4. The tertiary amine groups in the polymer backbone change from the deionized state to the ionized state when the pH decreases from 7.4 to 6.8. This makes the polymer change from amphiphilic to totally hydrophilic and thus makes the polymeric nanoparticles disassociate in aqueous solution. SPIONPs were encapsulated into these polymeric nanoparticles by a film hydration method. The as-prepared polymer-based nanobiosensor is stable at physiological pH (7.4) and body temperature (37°C) but can rapidly release the encapsulated nanoparticles once the pH is decreased to 6.8, leading to an enhanced accumulation of iron oxide in the acidic brain ischemic area. The *in vivo* $T_2$-weighted MR result shows a gradual accumulation of SPIONPs in the brain ischemic area. We also tested the imaging ability of our nanobiosensor system using tumor models. Compared with a non-pH-sensitive nanobiosensor system (iron oxide nanoparticles loaded in Pluronic F127), our pH-sensitive nanobiosensor can successfully give a clear image of the tumor. These results support the hypothesis that our pH-responsive nanobiosensor successfully targets acidic pathological tissues and provides a clear image of them. Subsequently, we encapsulated an anticancer drug, DOX, into our nanobiosensor (13). An *in vitro* drug release experiment showed that the DOX release rate was also accelerated at lower pH, which makes it possible to achieve the simultaneous imaging and therapy of acidic tumors. In another work of our group, we synthesized an amphiphilic diblock copolymer with polypeptides bearing tertiary amine groups and fabricated core/shell-structured nanoparticles for the delivery of SPIONPs (14). This nanobiosensor system can rapidly release SPIONPs in response to an acidic environment, which also improves the passive accumulation of SPIONPs in the brain ischemic area and results in strong MR signals (Fig. 2). Moreover, it exhibits long-term stability, low cytotoxicity and strong *in vivo* imaging of brain ischemic areas, which makes it a good candidate for the detection of cerebral ischemia.

Other groups also performed much good work in the MR imaging of acidic pathological areas using SPIONPs loaded in pH-sensitive polymeric nanocarriers with ionizable amine groups for tumor-targeted imaging. For example, Crayton and Tsourkas synthesized dextran-stabilized SPIONPs and employed glycol chitosan to prepare a pH-responsive nanobiosensor (34). Under acidic conditions, the surface charge of their nanobiosensor becomes positive, which increases its electrostatic interactions with the negatively charged cell membranes. This change could increase the retention of the nanobiosensor at the tumor site. *In vivo* experiments demonstrated that, compared with non-pH-sensitive nanoparticles, their pH-sensitive nanobiosensor showed a significantly improved accumulation in a murine tumor model, which resulted in a clear magnetic resonance contrast in $T_2$-weighted images. Using a pH-sensitive polymer bearing tertiary amine groups (PEG-*block*-PDPA), Gao and his coworkers prepared a nano

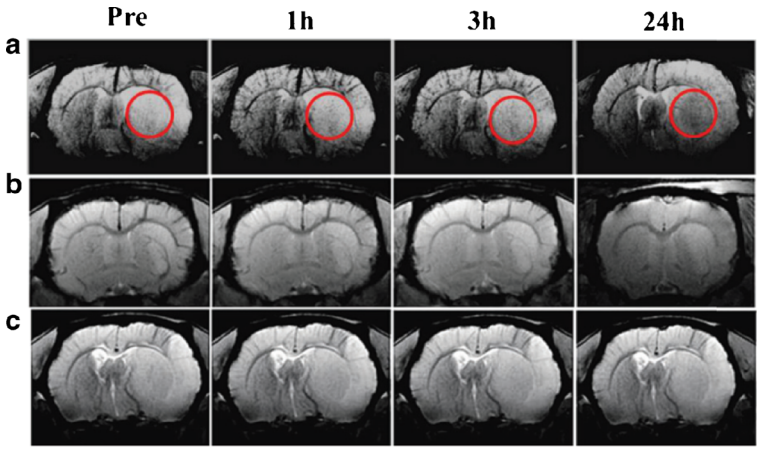


**Fig. 2** $T_2$-weighted MR image of rat brains obtained from (**a**) SPIONPs-loaded pH-sensitive nanobiosensors, (**b**) SPIONPs-loaded non-pH-sensitive nanobiosensors, and (**c**) blank pH-senstive nanobiosensors as a control. This result showed that pH-sensitive nanobiosensors are effective in targeting brain ischemic areas. Reproduced with permission (14).

system for simultaneous imaging and therapy by encapsulating SPIONPs and β-lap (an anticancer drug) into this polymer (35). This nano system can be internalized into acidic organelles and responds to the acidic environment, leading to improved therapeutic efficacy in cancer cells. In addition to polymers bearing ionizable amine groups, polymers bearing acid-labile groups were also employed by researchers for the physical encapsulation of SPIONPs. Lu et al. synthesized an amphiphilic polymer with acid-labile bonds in its hydrophobic pendent groups (32). A pH-sensitive nanobiosensor was prepared by loading SPIONPs into self-assembled nanoparticles of this polymer. A significant decrease of the $T_2$-weighted intensity of this nanobiosensor was observed in an acidic environment, owing to the partial aggregation of the hydrophobic SPIONPs at lower pH. This decrease of the $T_2$-weighted intensity raised the sensitivity and detectability of this nanobiosensor in MR imaging.

In addition to enhanced tumor-targeted imaging using pH-sensitive nanobiosensors, some researchers also studied polymer-based MR imaging nanobiosensors with pH-dependent drug release for simultaneous imaging and therapy. For example, Yan et al. reported a composite nanobiosensor with DOX and PEG chemically conjugated onto SPIONPs (36). DOX release from this composite nanobiosensor is accelerated upon exposure to an acidic environment due to the cleavage of the acylhydrazone linkages between DOX and the SPIONPs. *In vivo* MR images of tumor tissues confirmed the possibility of using this nanocomposite for cancer theranostics (Fig. 3). Cao et al. reported a nano system prepared by coating tertiary amine-containing polymers onto SPIONPs (37). Two chemical drugs, chlorambucil and indomethacin were used as model drugs and were physically loaded into this nano system. Magnetization curves and pH-dependent drug release behaviors indicated that this nano system can be used for imaging and therapy. Wang et al. prepared a nano system with SPIONPs coated by an anionic polymer, PAA (38). DOX was loaded into this nano system by the electrostatic interactions between DOX and PAA. Magnetic hysteresis curves show the capability of this nano system for MR imaging, and the pH-dependent DOX release shows that it can be used to treat acidic cancers. Lu et al. reported the co-encapsulation of SPIONPs, hollow

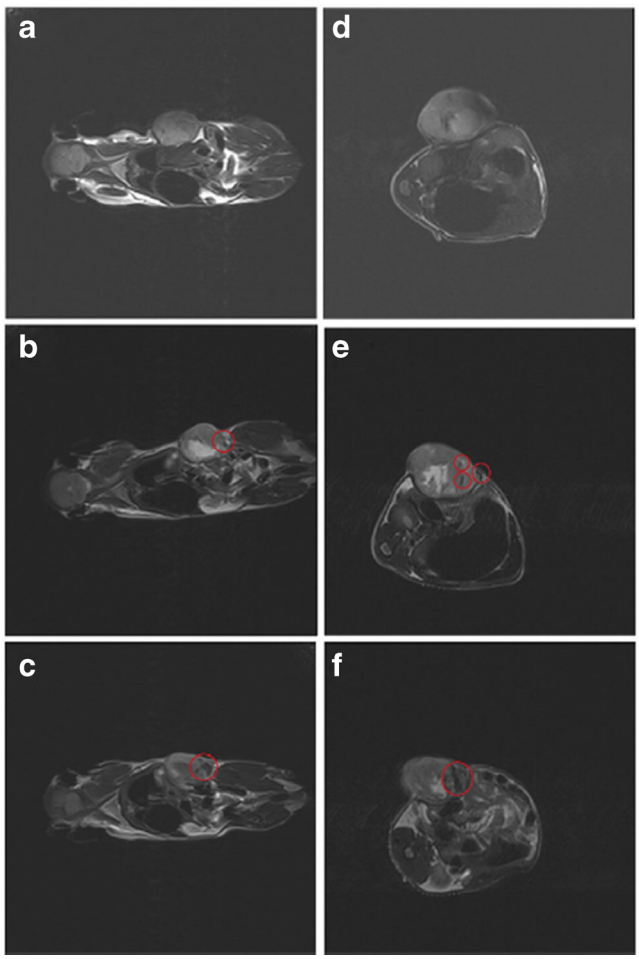


**Fig. 3** $T_2$-weighted coronal (**a**, **b**, **c**) and transversal cross-sectional (**d**, **e**, **f**) MR images of tumor-bearing mice pre-injection (**a**, **d**), at 30 min (**b**, **e**) and at 120 min (**c**, **f**) after intravenous injection of a SPIONP-incorporated pH-sensitive nanobiosensor. The position of the dark region in tumor was marked by red circles. Reproduced with permission (36).

mesoporous silica and DOX by a pH-sensitive polymer synthesized by reversible addition–fragmentation chain transfer polymerization (39). This multi-functional nano system could both facilitate drug release under acidic conditions (due to its cleavage of acid-labile acetal bonds) and track the cancer targeting process (due to its magnetism).

Paramagnetic $Gd^{3+}$ complexes are the most widely used $T_1$ contrast agents for MR imaging because of their enhanced relaxation (2,40). To lower the toxicity, the chelation of $Gd^{3+}$ with ligands (such as DOTA) is more commonly employed than free $Gd^{3+}$. By chemically linking DOX, folic acid and DOTA-Gd onto β-CD based star copolymers, Liu and his coworkers prepared multifunctional pH-responsive nanoparticles with both imaging and therapy abilities (41). The DOX release from these nanoparticles was dramatically accelerated at pH 5.0 and 4.0 compared to that at pH 7.4, owing to the cleavage of acid-labile bonds at a lower pH. Time-dependent MR images recorded for a normal rat showed that these nanoparticles are mostly accumulated in the kidney. Kikuchi et al. utilized the morphology changes of a pH-sensitive polymer to prepare nanobiosensors containing $Gd^{3+}$ with switchable properties (42). Relaxivity measurements showed that their nanobiosensors have molecular switches that respond to pH changes due to the alteration of the molecular tumbling caused by pH-responsive morphological changes. Also based on the pH-responsive morphological changes of polymers, in another work of Kikuchi and his coworkers, they reported ratiometric MR imaging sensors for quantitative pH imaging (43).

In addition to the above-mentioned SPIONPs and $Gd^{3+}$-containing nanobiosensors, polymer-based and pH-sensitive nanobiosensors have been prepared by the self-assembly of polymers copolymerized by monomers bearing tertiary amines and $^{19}F$. Gao et al. prepared $^{19}F$-conjugated amphiphilic polymers with appropriate pKa values for sensing the pH difference between normal tissues and tumor tissues (44). At pH 7.4, this polymer forms core-shell structured nanoparticles and exhibits a very weak MR signal; however, the MR signal is activated when the pH is decreased to 5.0 due to the disassociation of the nanoparticles caused by the ionization of tertiary amine groups. Compared to small molecular pH sensors, the pH response of their nanobiosensors is extremely sharp, which allows for a qualitative measurement of tumor pH values. Using a similar principle, Whittaker and his coworkers designed and prepared a pH-activatable $^{19}F$-containing MR imaging contrast agents for tumor-selective imaging (45).

Interestingly, Gao and his coworkers reported that ionizable tertiary amine-containing polymers can be used as pH-responsive contrast agents for MR imaging (46). The signal is "off" when the polymers form nanoparticles at pH 7.4 but is activated to the "on" state when they dissolve at lower pH.

## Polymer-Based and PH-Sensitive Nanobiosensors for Fluorescence Imaging

Fluorescent nanoparticles, especially stimulus-sensitive fluorescent nanoparticles, have been widely employed for many biomedical applications, including bioimaging and pH sensing (47–51). Among these fluorescent nanoparticles, polymer-based pH-sensitive nanobiosensors showed many unique properties and functions. So far, most of the polymer-based pH-sensitive nanobiosensors for fluorescence imaging have been prepared by a combination of fluorescent molecules or quantum dots with pH-sensitive polymers (52–54). However, polymer-based pH-sensitive nanobiosensors for fluorescence imaging could also be prepared by the self-assembly of conjugated polymers with pH-sensitivity (55).

It is well known that several factors (such as energy transfer and complex formation) might cause quenching of fluorescent groups. Fluorescent probes that are "turned off" at physiological pH but can be "turned on" at lower pH are of particular interest for cancer diagnosis (56). Our group first reported a series of TRITC-loaded biodegradable and biocompatible pH-sensitive polymeric nanoparticles that can be used as imaging agents for tumor diagnosis (52). These polymeric nanoparticles are stable in aqueous solution when the tertiary amine groups of these polymers are deionized at higher pH but are destroyed when they are ionized at lower pH. This demicellization/micellization transformation behavior leads to an "ON/OFF" change of fluorescent TRITC. It is found that the activation pH of fluorescence can be successfully controlled by controlling the pH-sensitivities of the polymers. *In vitro* cell uptake experiments showed that the pH-dependent fluorescence signals of these nanoparticles in cultured cells are consistent with our expectations; below the demicellization pH values, quenched TRITC was released from the polymeric nanoparticles and rapidly taken up by cells, resulting in a strong fluorescence signal. *In vivo* fluorescence imaging experiments in tumor-bearing mice indicated that only a polymer with appropriate pH sensitivity can give a clear image of a tumor, and this image is superior to that obtained from a non-pH-sensitive polymer (Fig. 4). With this principle, we encapsulated a photosensitizer, PpIX, into our pH-sensitive polymeric nanoparticles and tested this system for *in vivo* tumor diagnosis and photodynamic therapy (57). This PpIX-loaded polymeric nanobiosensor has good stability at physiological pH, appropriate size for EPR-mediated accumulation and sharp pH-dependent disassociation that enables the rapid release of PpIX at weakly acidic tumoral conditions. In tumor-bearing mice, these nanoparticles showed not only clear fluorescent imaging of the tumors but also complete inhibition of the tumors. These results indicated that our PpIX-loaded polymeric nanoparticles enable simultaneous tumor diagnosis and therapy and have great potential for the clinical treatments of various tumors. In another work of our

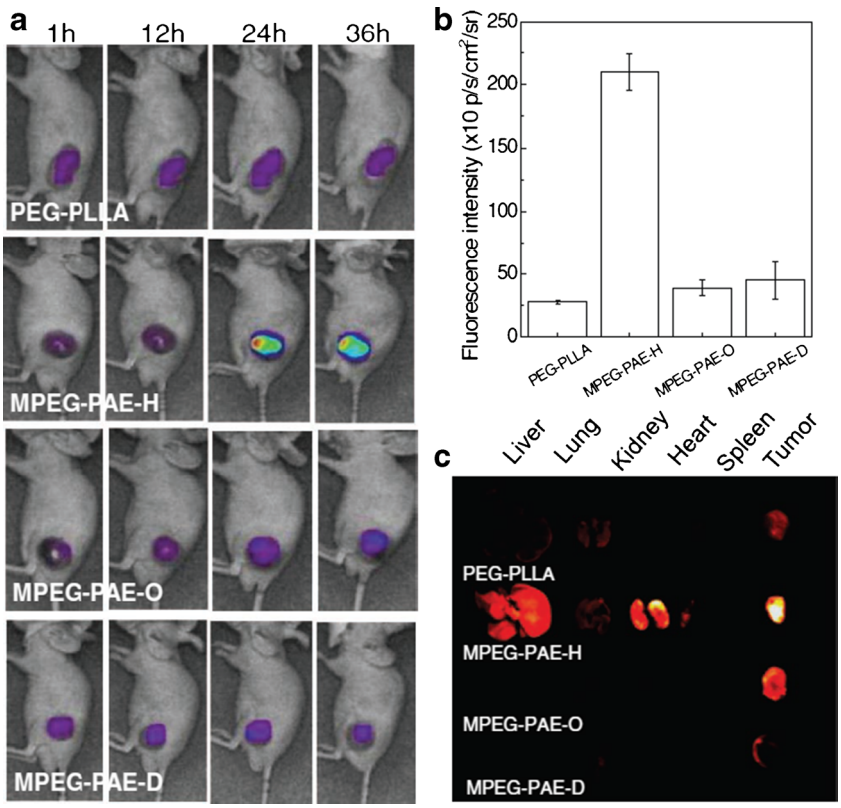


**Fig. 4** Fluorescence imaging results of tumor-bearing mice. **a** Fluorescence images of a non-pH-sensitive nanobiosensor and nanobiosensors with different pH-sensitivities. **b** Quantification of fluorescence recorded for each tumor at 1 day post-injection ($n = 3$). **c** *In vitro* fluorescence images of dissected organs of tumor-bearing mice sacrificed at 2 days post-injection. Reproduced with permission (52).

group, we conjugated a tumor-targeting peptide onto our pH-sensitive polymeric nanoparticles and encapsulated TRITC and DOX into these nanoparticles (15). An *in vivo* fluorescence image of tumor-bearing mice showed that the fluorescence signals from tumor-targeting peptide-conjugated pH-sensitive polymeric nanoparticles are much stronger that those from pH-sensitive polymeric nanoparticles without conjugation of a tumor-targeting peptide, indicating their enhanced tumor-targeting ability. This enhanced tumor targeting also leads to the enhanced anti-tumor efficacy of these TRITC and DOX-loaded pH-sensitive polymeric nanoparticles.

By controlling the pH-dependent micellization/demicellization behaviors of tertiary amine-containing and fluorescent dye-conjugated diblock copolymers, Gao and his coworkers performed a series of interesting works on polymeric nanobiosensors with a sharp and tunable activation pH of fluorescence (16,53,58,59). In their research, TMR (a pH-insensitive fluorescent dye) was employed as a model fluorophore and was conjugated to the pH-sensitive block of their diblock copolymer to investigate the pH-responsive fluorescence activation of the nanobiosensors (16). Above the pKa values of the tertiary amine groups, the copolymers are amphiphilic and form self-assembled nanoparticles in aqueous solution, which quenches the fluorescence of the TMR groups due to the aggregation of the hydrophobic blocks. However, when the pH was decreased to below the pKa values of the tertiary amine groups, the tertiary amine groups on the hydrophobic blocks became ionized, making the copolymer change from amphiphilic to completely hydrophilic; this change broke down the nanostructure of the copolymers and led to a significant increase in the fluorescence intensity. Further confocal imaging studies showed that the nanobiosensors are inactive before being taken up by cells (pH 7.4 media) but become active immediately once they are taken up by cells. More interestingly, nanobiosensors with different fluorescence activation pH values can be selectively activated in endocytic compartments with different pH values, such as early endosomes (pH 5.9–6.2) and lysosomes (pH 5.0–5.5). Gao and his coworkers further developed fluorescent nanobiosensors with multichromatic emissions using their pH-sensitive copolymers (58). In this work, pH-insensitive dyes with fluorescent emissions from green to near infra-red were conjugated to the pH-sensitive blocks of copolymers with different pH-sensitivities, and then all the dye-conjugated polymers were self-assembled to prepare multicolored nanobiosensors with a tunable activation pH of fluorescence (pH 5.2, 6.4, 6.9 and 7.2) and a wide range of emission wavelengths (500–820 nm). Time-dependent confocal images of human H2009 lung cancer cells after incubation with a mixture of different nanobiosensors indicated the step-by-step activation of the nanobiosensors (nanobiosensors with higher activation pH of fluorescence are activated earlier than those with a lower activation pH) inside endocytic compartments. They then expanded their concept to a library of ultra nanobiosensors with a predictable activation pH of fluorescence and wider fluorescent emission wavelengths (400–820 nm) based on

standard curves (59). This nanobiosensor library consists of ten types of nanoparticles and covers the entire physiologic pH range (pH 4.0–7.4) in 0.3 pH increments, providing good opportunities for translational studies in tumor imaging and drug delivery (Fig. 5). Finally, they tested the tumor imaging ability of their pH-activatable nanobiosensors on 10 different tumor models (53). In all the tumor models, the nanobiosensors were activated in the tumor microenvironment over normal tissues and organs (Fig. 6), indicating that these pH-sensitive nanobiosensors can not only successfully target the tumor microenvironment but also are promising in *in vivo* tumor imaging and therapy.

In addition to our group and Gao's group, other research groups have also reported interesting work on polymer-based nanobiosensors with pH-dependent fluorescence activation or pH-dependent emission intensity changes. For example, Wang et al. synthesized amphiphilic graft copolymers composed of PEG and pH-sensitive PAE and encapsulated a fluorescent dye, bis(pyrene), into the nanoparticles formed by these graft copolymers (60). Cell experiments showed that the pH-sensitive polymeric nanoparticles successfully delivered bis(pyrene) into the lysosomes of living cells via endocytosis. Due to the acidic nature of lysosomes, bis(pyrene) molecules were released from the disassociated polymeric nanoparticles and self-aggregated

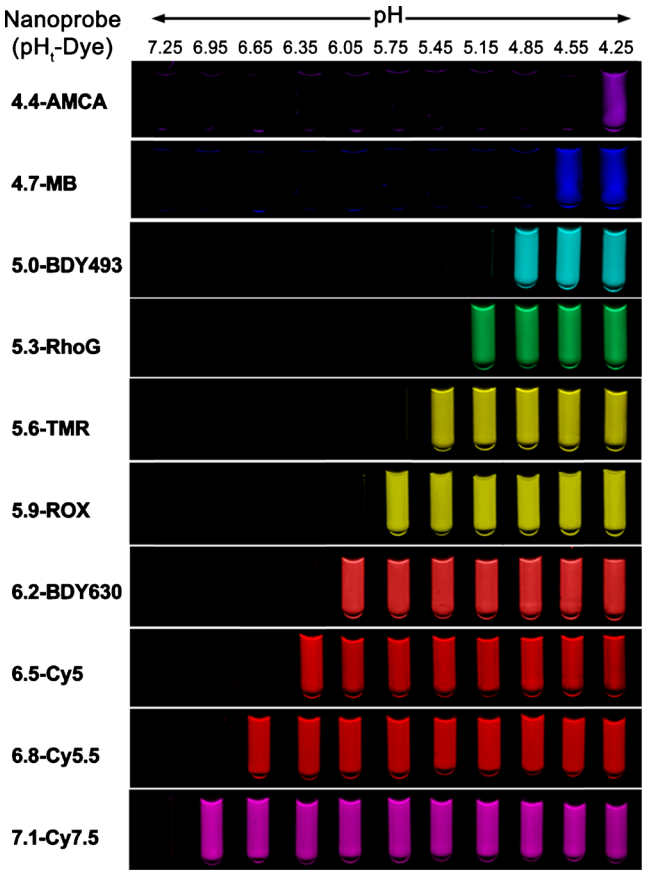


**Fig. 5** Fluorescence photographs showing a pH-sensitive nanobiosensor library with broad pH tunability (pH 4–7.4) and fluorescence emissions (400–820 nm). Reproduced with permission (59).

*in situ*, causing the activation of fluorescence emissions inside HeLa cells as observed from spinning disk confocal microscopy images. Bojinov and his coworkers reported polymer-based and pH-sensitive nanobiosensors formed by the self-assembly of a dye-conjugated poly(methyl methacrylate)-*block*-poly(methacrylic acid) diblock copolymer (61). The emission intensity of the as-formed nanobiosensors is highly sensitive to pH changes, with a remarkable intensity increase when the pH is decreased from 5 to 3. These nanobiosensors could be internalized by HeLa cells and showed much higher photo-stability than the pure organic dyes. Wolfbeis and his coworkers reported on a nanobiosensor system for the imaging of pH values in living cells (62). This system has a core made from a commercially available biocompatible polymer, Pluronic F-127, and a shell made from PEG conjugated with a pH-sensitive probe. The emission intensity of the nanobiosensor steadily increased with the increasing solution pH (from pH 3 to 9). The core/shell-structured nanobiosensor is stable in aqueous media and can be internalized into the cellular cytosol by electroporation, which enables the sensing and imaging of pH values inside cells. Liu and his coworkers reported a polyethyleneimine-based fluorescent nanobiosensor that can be activated in acidic tumor environments (63). When the pH is decreased from 7.4 to 6.5, the surface charge of their nanobiosensor switched from negative to positive, and then the electrostatic interactions between the positively charged nanobiosensor and negatively charged cell membranes "light up" the fluorescence of the dye, which allows for cancer cell imaging.

Although most of the polymer-based and pH-sensitive fluorescent nanobiosensors reported so far have pH-dependent fluorescent properties, polymer-based and pH-sensitive fluorescent nanobiosensors with pH-dependent drug release have also been reported. Yan et al. conjugated a near infra-red dye and DOX onto a polypeptide-based copolymer and fabricated a nanobiosensor with it (64). The DOX release rate was accelerated at pH 5.4 compared to that at pH 7.2 due to the cleavage of the hydrazone bond between DOX and the polypeptide. Confocal laser scanning microscopy images showed a fast and enhanced endocytosis of the nanobiosensor by cells, indicating the possibility of using this nanobiosensor as a candidate for cancer theranostics.

Quantum dots have been extensively studied by researchers for bioimaging applications due to their high quantum yields, tunable emission spectrum and outstanding photostability (48,65–67). Among these studies, some work focused on the fabrication and evaluation of pH-sensitive polymer/quantum dot nanocomposites. For example, Shuai and his coworkers reported a multifunctional pH-sensitive nano system for tumor-targeted intracellular drug release and fluorescent imaging (54). This nano system is composed of a paclitaxel- and quantum dot-encapsulated pH-sensitive core and a folic acid-conjugated PEG shell. Drug loss was almost completely inhibited at pH 7.4, while the drug release rate was significantly increased at pH 5.0. *In vivo* experiments in tumor-

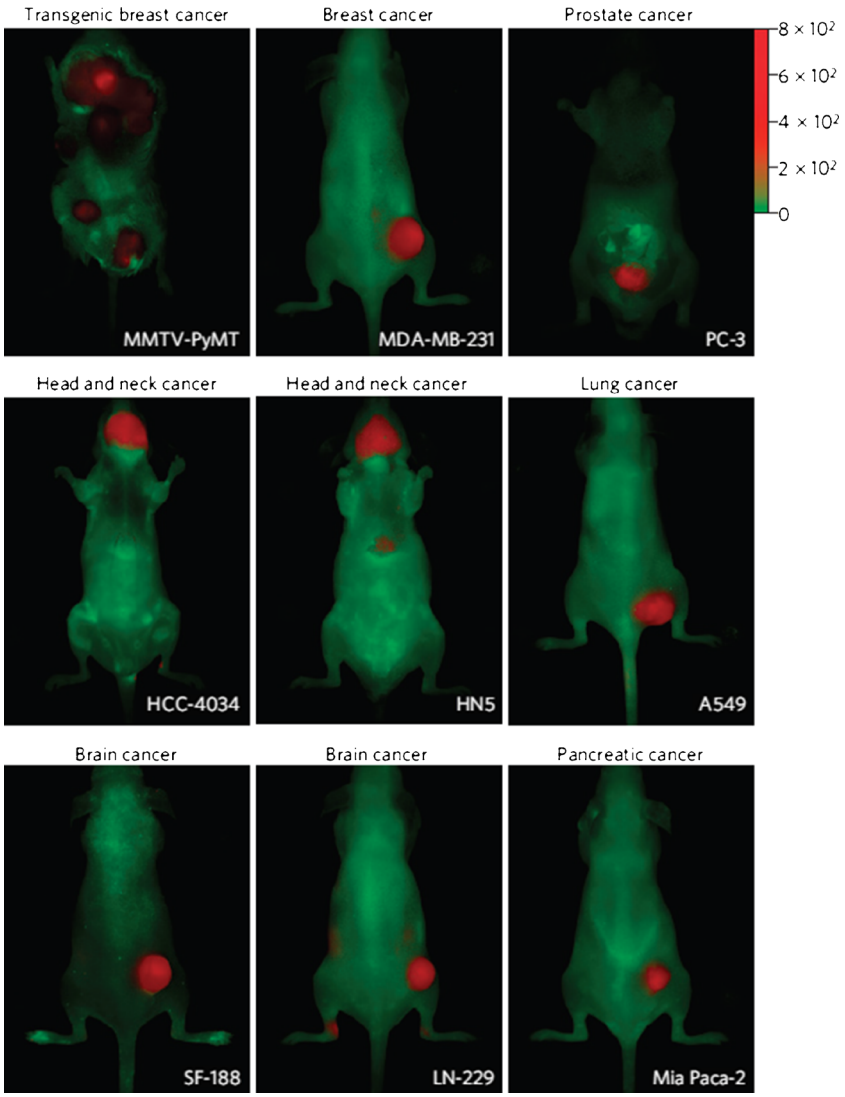


**Fig. 6** Fluorescence images showing broad tumor imaging specificity and efficacy of pH-sensitive nanobiosensors in 10 different tumor models of different cancer types (breast, prostate, head and neck, lung, brain and pancreatic cancers). Reproduced with permission (53).

bearing mice verified that this multifunctional nano system is not only powerful in the diagnosis of tumors but is also promising in the inhibition of tumor growth. Zhang et al. prepared a core/shell-structured nanobiosensor system by chemically linking PEG with a 9-poly-D-arginine/CdTe nanocomposite through a pH-sensitive hydrazone bond for the delivery of siRNA to tumor cells (68). The breakage of the hydrazine bonds in the acidic tumor environment induced the detachment of the PEG shell and thus exposed the 9-poly-D-arginine/CdTe nanocomposite. The remaining 9-poly-D-arginine/CdTe nanocomposite has a high cell-penetrating ability, which can enhance cellular uptake and improve the intracellular delivery of siRNA. *In vivo* imaging results showed that, compared with nanobiosensors consisting of the same components but lacking the pH-sensitive hydrazone bond, this pH-sensitive nanobiosensor system is more powerful in the fluorescence imaging of tumor tissues (higher fluorescence intensity from tumor tissues was observed). Li et al. fabricated quantum dot-loaded nanogels with pH-sensitive fluorescence for cell imaging and drug delivery (69). The fluorescence intensities of the quantum dot-loaded nanogels gradually increased with the increasing solution pH (from 6.7 to 10.5), and their cytotoxicity was much lower than that of free quantum dots. Incorporation of an anticancer drug (methotrexate) into the nanogels makes it possible to use this system for cancer theranostics.

Semiconducting polymer dots are a novel class of fluorescent nanobiosensors that has aroused great research interest in recent years because of their high brightness, rapid emission rate and good photo-stability (70–73). Polymer dots are aggregates of π-conjugated polymers of small particle size that have exhibited many unique properties in bioimaging. Semiconducting polymer dots with pH-sensitivity were prepared by Chiu and his coworkers for ratiometric pH sensing (55). In this work, they adopted three methods to covalently conjugate a pH-sensitive dye, fluorescein, onto a non-pH-sensitive and conjugated polymer, poly(2,5-di(3′,7′-dimethyloctyl)phenylene-1,4-ethynylene), and finally obtained

three pH-sensitive polymer dots. All three types of polymer dots exhibited a ratiometric sensing capability with a linear pH sensing range between pH 5 and 8, which makes them suitable for most bioimaging studies.

DOX is one of the most commonly used chemo-therapeutic drugs and has a fluorescence emission wavelength ranging from 535 to 650 nm (74). Owing to the inherent fluorescence of this molecule, besides serving as an anticancer agent in a polymer-based and pH-sensitive nano drug delivery system, it has also been extensively used to observe the cellular uptake behaviors of these nano systems *in vitro* (75–79). Because of limitations of length, it will not be discussed in detail in this text.

### Polymer-Based and PH-Sensitive Nanobiosensors for MR and Fluorescence Dual Imaging

Because each imaging technique has its own strengths and weaknesses (for example, optical fluorescence imaging is difficult to be quantified, especially in tissues more than a few millimeters in depth, and MR imaging has high resolution but low sensitivity), the combination of two different imaging techniques might provide better diagnostic and therapeutic abilities (80–83). Nanobiosensors that offer dual MR/fluorescence imaging functions are the most widely studied in academic research and clinical applications. To date, several research papers have been published related to polymer-based and pH-sensitive nanobiosensors for MR and fluorescent dual imaging, and some of these nanobiosensors have been evaluated *in vivo*.

By encapsulating SPIONPs into pH-sensitive red fluorescent dye (sulforhodamine 101)-conjugated polymeric nanoparticles (formed from PEG-*block*-PAE polymer), our group first reported a polymer-based and pH-sensitive nanobiosensor for MR and fluorescent dual imaging (84). This nanobiosensor showed concentration- and pH-dependent fluorescence emission intensity and could rapidly release SPIONPs in response to the tumor extracellular pH. Relaxation property assessments demonstrated that this nanobiosensor can be used as a $T_2$-weighted MR imaging contrast agent. This report provided a good example of a polymer-based and pH-sensitive nanobiosensor that contains iron oxide nanoparticles and small fluorescent molecules for MR and fluorescent dual imaging. Hyeon and his coworkers provided another example by the preparation of a multifunctional tumor pH-sensitive nano system with dual imaging capabilities (85). This multifunctional system consists of a pH-sensitive polymer, extremely small iron oxide nanoparticles as a MR contrast agent, and chlorin e6 as a photosensitizer. This system is able to target tumors via the surface-charge reversal in response to the acidic tumor pH (pH 6.5–7.0). Further decreases in the pH (pH < 6.5) can trigger the disassembly of this multifunctional system and then active MR contrast, fluorescence and photodynamic therapeutic ability. *In vivo* experiments on tumor-bearing mice indicated that this nano system not only enables the dual-modal imaging of small tumors but also shows good anti-tumor efficacy.

Polymer-based and pH-sensitive nanobiosensors with MR and fluorescent dual imaging capabilities were also fabricated by using $Gd^{3+}$ as a MR contrast agent and small fluorescent molecules as a fluorescent probe. For example, Liu and his coworkers reported core-crosslinked pH-swellable polymeric nanoparticles that are covalently labeled with DOTA-Gd complex and NBD (a green light-emitting dye) (86). Compared with non-crosslinked precursor nanoparticles, the core-crosslinked nanoparticles exhibited better MR and fluorescence imaging ability due to their structural stability and integrity. Under mildly acidic conditions, both the MR and fluorescence imaging signals were enhanced, indicating that this system is a good candidate for the dual imaging of acidic tumors. Na and his coworkers prepared a Cy5.5- (a fluorescent dye) and $Gd^{3+}$-containing nanobiosensor from a pH-sensitive polymer with cancer-recognizing ability (87). The fluorescence signals of this nanobiosensor gradually increased in the tumor region from 30 min to up to 2 h post-injection. This nanobiosensor also exhibits strong $T_1$ MR signals in the acidic tumoral environment, which enables the detection of small tumors.

Liu et al. synthesized $Mn^{2+}$-doped charge-reversal nanoparticles with strong red light emission at approximately 660 nm for imaging-guided pH-sensitive photodynamic therapy (88). The surface of these nanoparticles is negatively charged and PEG coated at pH 7.4 and could be converted to positively charged at pH 6.8 by the cleavage of the amide bond. This conversion enhances the cell uptake of the nanoparticles and thus increases their *in vitro* photo dynamic therapy efficacy. Owing to their intrinsic optical and paramagnetic properties, these nanoparticles have shown promising *in vivo* results as dual-modal imaging agents.

## POLYMER-BASED AND PH/TEMPERATURE DUAL-SENSITIVE NANOBIOSENSORS

Dual-sensitive, especially pH/temperature dual-sensitive, polymeric nanoparticles are of great importance in efficient drug delivery and bioimaging (89–92). Normally, the temperature in a living body is 37°C; however, elevated temperature could be caused by a disease or an external signal. PNIPAm, with an LCST of approximately 33°C (which means that it is soluble in water below 33°C but insoluble and causes phase separation in water above 33°C), is the most frequently used polymer in the construction of temperature-sensitive nanoparticles. The LCST of PNIPAm can be tuned by copolymerization with a more hydrophilic or a more hydrophobic monomer. Pluronic F127 is another popular temperature-sensitive polymer.

Perhaps because of the complexity of dual-sensitive nanobiosensors, there are not many successful reports regarding these systems. Reports with *in vivo* results in this research topic

are even fewer. Considering that dual stimuli-sensitive nanobiosensors are more powerful that single stimulus-sensitive nanobiosensors, we believe that more studies will be conducted and more fruitful results will be made in this field in the near future.

### Polymer-Based and PH/Temperature Dual-Sensitive Nanobiosensors for MR Imaging

Wadajkar et al. reported the synthesis of a dual-sensitive polymer with PNIPAm as a building block and the fabrication of dual-sensitive polymer-coated SPIONPs for targeted drug delivery and bioimaging (93). DOX release from these polymer-coated SPIONPs is both temperature- and pH-dependent (with a faster release at pH 6 than at pH 7.4 and a faster release at 40°C than at 37°C). The cellular uptake of these polymer-coated SPIONPs was also significantly increased in the presence of a 1.3 T magnetic field. Pramanik et al. reported magnetic nanocomposites made from the modification of ferrite nanoparticles with a pH/temperature dual-sensitive copolymer for cancer therapy and MR imaging (94). A DOX release study at different pH and temperatures showed that the DOX release rate is the fastest at pH 5.5 and body temperature. $T_2$-weighted MR images of HeLa cells incubated with the nanocomposites showed a notable contrast enhancement, indicating the uptake of the nanocomposites by cells.

### Polymer-Based and PH/Temperature Dual-Sensitive Nanobiosensors for Fluorescence Imaging

Qian et al. developed a polymeric fluorescent nanobiosensor that contains PNIPAM as a building block (95). Because this nanobiosensor is responsive to pH/temperature dual stimuli, it was evaluated as an intracellular pH sensor for lysosome imaging and a temperature sensor for temperature changes in living cells. Zhuo and his coworkers prepared polyion complex micelles from a positively charged polymer and a negatively charged polymer (both polymers are pH- and temperature-sensitive) (96). Next, these polyion complex micelles were endowed with fluorescent properties by introducing two different fluorescent dyes. Photographs of these micelles and confocal laser scanning images of HeLa cells treated with these micelles show that these dye-labeled micelles exhibit temperature- and pH-dependent fluorescence, which makes them promising for the bioimaging of tumor microenvironments.

Zhou and his coworker reported several pH/temperature dual-sensitive fluorescent hybrid nanogels for cancer cell imaging and controlled drug delivery (97–99). Their hybrid nanogels are generally comprised of an inorganic core (CdSe quantum dots or silver nanoparticles) and a crosslinked and pH/temperature-sensitive polymeric shell. These hybrid nanogels exhibit temperature- and pH-dependent size in aqueous solutions and also pH-dependent fluorescence intensity and drug release behavior. Given the good biocompatibility of these hybrid nanogels, they are very promising for the targeted delivery of imaging agents and the controlled release of drugs to tumor tissues.

## POLYMER-BASED AND PH/TEMPERATURE DUAL-SENSITIVE NANOBIOSENSORS FOR MR/FLUORESCENCE DUAL IMAGING

Yang et al. reported pH/temperature dual-sensitive magnetic nanogels conjugated with Cy5.5-labeled lactoferrin for the MR/fluorescence dual imaging of a brain tumor (100). In response to different pH and temperatures, these dually sensitive nanogels change in their size and hydrophilic/

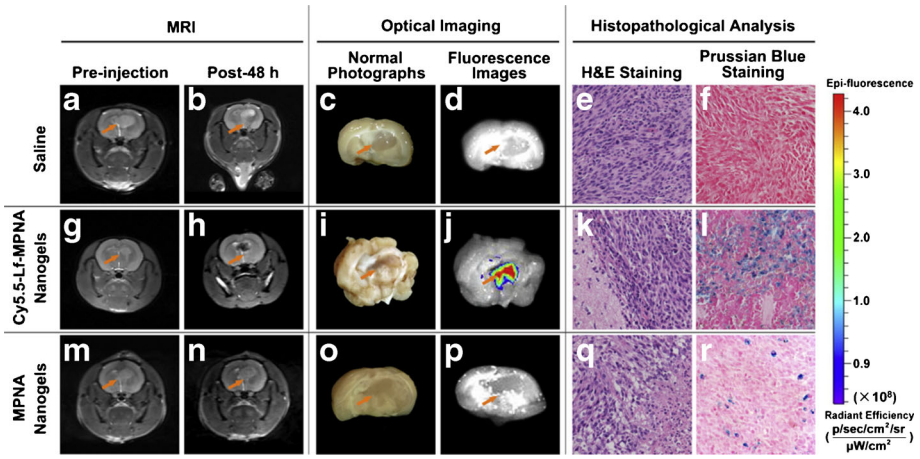


**Fig. 7** Animal experiment results of gliomas-bearing rats treated with saline as a control (*upper row*), Cy5.5-labled lactoferrin-conjugated nanobiosensor (*middle row*), and non-conjugated nanobiosenor (*lower row*), respectively. $T_2$-weighted MR Images of gliomas before injection (**a**, **g**, **m**) and at 48 h post-injection (**b**, **h**, **n**); normal photographs (**c**, **i**, **o**) and *ex vivo* fluorescence images (**d**, **j**, **p**) of gliomas at 48 h post-injection; histological sections of gliomas with H&E staining (**e**, **k**, **q**) and Prussian blue staining (**f**, **l**, **r**). Reproduced with permission (100).

**Table I** Summary of Polymer-Based and pH-Sensitive Nanobiosensors for Theranostics

| | Environment responsiveness | Method of Imaging | Imaging Agents | Therapeutic agents | *In vivo* results | Ref. |
|---|---|---|---|---|---|---|
| 1 | pH-sensitive | MR imaging | SPIONPs | N/A | Yes | (12) |
| 2 | pH-sensitive | MR imaging | SPIONPs | DOX | Yes | (13) |
| 3 | pH-sensitive | MR imaging | SPIONPs | DOX | Yes | (14) |
| 4 | pH-sensitive | MR imaging | SPIONPs | – | Yes | (34) |
| 5 | pH-sensitive | MR imaging | SPIONPs | β-lap | No | (35) |
| 6 | pH-sensitive | MR imaging | SPIONPs | DOX | No | (32) |
| 7 | pH-sensitive | MR imaging | SPIONPs | DOX | Yes | (36) |
| 8 | pH-sensitive | MR imaging | SPIONPs | Chlorambucil and indomethacin | No | (37) |
| 9 | pH-sensitive | MR imaging | SPIONPs | DOX | No | (38) |
| 10 | pH-sensitive | MR imaging | SPIONPs | DOX | No | (39) |
| 11 | pH-sensitive | MR imaging | $Gd^{3+}$ | DOX | Yes | (41) |
| 12 | pH-sensitive | MR imaging | $Gd^{3+}$ | – | No | (42) |
| 13 | pH-sensitive | MR imaging | $Gd^{3+}$ | – | No | (43) |
| 14 | pH-sensitive | MR imaging | $^{19}F$ | – | No | (44) |
| 15 | pH-sensitive | MR imaging | $^{19}F$ | – | No | (45) |
| 16 | pH-sensitive | MR imaging | Tertiary amine-containing polymer | – | No | (46) |
| 17 | pH-sensitive | Fluorescence imaging | TRITC | – | Yes | (52) |
| 18 | pH-sensitive | Fluorescence imaging | PpIX | PpIX | Yes | (57) |
| 19 | pH-sensitive | Fluorescence imaging | TRITC | DOX | Yes | (15) |
| 20 | pH-sensitive | Fluorescence imaging | TMR, Cy5.5, RhoG, ROX, BDY, etc. | – | Yes | (16,53,58,59) |
| 21 | pH-sensitive | Fluorescence imaging | Bis(pyrene) | – | No | (60) |
| 22 | pH-sensitive | Fluorescence imaging | 1,8-naphthalimide/rhodamine pair | – | No | (61) |
| 23 | pH-sensitive | Fluorescence imaging | Fluorescein | – | No | (62) |
| 24 | pH-sensitive | Fluorescence imaging | TPS | – | No | (63) |
| 25 | pH-sensitive | Fluorescence imaging | Cyanine | DOX | No | (64) |
| 26 | pH-sensitive | Fluorescence imaging | CdSe/ZnS quantum dots | Paclitaxel | Yes | (54) |
| 27 | pH-sensitive | Fluorescence imaging | CdTe quantum dots | siRNA | Yes | (68) |
| 28 | pH-sensitive | Fluorescence imaging | CdTe quantum dots | Methotrexate | No | (69) |
| 29 | pH-sensitive | Fluorescence imaging | Conjugated polymer dots | – | No | (55) |
| 30 | pH-sensitive | MR and fluorescence dual imaging | SPIONPs and Sulforhodamine 101 | – | No | (84) |
| 31 | pH-sensitive | MR and fluorescence dual imaging | Extremely small iron oxide nanoparticles and Chlorin e6 | Chlorin e6 | Yes | (85) |
| 32 | pH-sensitive | MR and fluorescence dual imaging | $Gd^{3+}$ and NBD | – | No | (86) |
| 33 | pH-sensitive | MR and fluorescence dual imaging | $Gd^{3+}$ and Cy5.5 | – | Yes | (87) |
| 34 | pH-sensitive | MR and fluorescence dual imaging | $Mn^{2+}$ and Chlorin e6 | Chlorin e6 | Yes | (88) |
| 35 | pH/temperature dual sensitive | MR imaging | SPIONPs | DOX | No | (93) |
| 36 | pH/temperature dual sensitive | MR imaging | SPIONPs | DOX | No | (94) |
| 37 | pH/temperature dual sensitive | Fluorescence imaging | $A_4$ | – | No | (95) |
| 38 | pH/temperature dual sensitive | Fluorescence imaging | 5-aminofluorescein and Rhodamine B | – | No | (96) |
| 39 | pH/temperature dual sensitive | Fluorescence imaging | CdSe quantum dots | Temozolomide | No | (97,98) |
| 40 | pH/temperature dual sensitive | Fluorescence imaging | Silver nanoparticles | Dipyridamole | No | (99) |
| 41 | pH/temperature dual sensitive | MR and fluorescence dual imaging | SPIONPs and Cy5.5 | – | Yes | (100) |
| 42 | pH/temperature dual sensitive | MR and fluorescence dual imaging | SPIONPs and RITC | DOX | No | (101) |

hydrophobic balance. Under physiological conditions (pH 7.4 and 37°C), the nanogels are hydrophilic and in the swollen state, which is favorable for prolonged blood circulation. Under slightly acidic tumor conditions (pH 6.8 and 37°C),

the nanogels change to hydrophobic and shrunk in volume, which facilitates tumor accumulation and cell uptake. *In vivo* MR/fluorescence imaging studies demonstrated that the dual-sensitive nanogels are good candidates for the detection of brain tumors with high sensitivity and specificity (Fig. 7). Dhara et al. reported core/shell-structured and dye-labeled nanoparticles with a magnetic core coated by a pH/temperature dual-sensitive polymer shell for targeted drug delivery and cancer imaging applications (101). Magnetic property studies and fluorescence microscopy images have demonstrated the possibilities of using these nanoparticles for MR/fluorescence dual imaging, Moreover, these nanoparticles are able to target specific cells and selectively release loaded drugs at specific pH and temperatures.

## SUMMARY AND FUTURE CHALLENGES

Many efforts have been made during the last decade to develop polymer-based and pH-sensitive nanobiosensors for the efficient diagnosis and therapy of various diseases. Taking advantage of the development of imaging techniques, these multifunctional intelligent nano systems show great potential for future clinical use. In this review, we started by explaining the basic principles for the design and fabrication of polymer-based and pH-sensitive nanobiosensors and then introduced polymer-based pH-sensitive nanobiosensors for MR, fluorescence and MR/fluorescence dual imaging and provided examples. Finally, polymer-based nanobiosensors with pH/temperature dual sensitivities were also covered. Table I summarizes most of the important reports in this research field from the last 5 years.

On the basis of the achievements that we have attained, future work should focus on the points listed below: (1) fabrication of nanobiosensors by a simple, safe and repeatable method, (2) understanding of different biological processes that are related to the delivery procedure, (3) multifunctionalization of nanobiosensors for more efficient delivery (including conjugation of active targeting groups, multiresponsiveness and co-delivery of multiple imaging and therapeutic agents), and (5) customized design for specific diseases. We believe that more and more valuable achievements will be made through the talents and continued efforts of researchers.

## ACKNOWLEDGMENTS AND DISCLOSURES

This manuscript was supported by the Basic Science Research Program through a National Research Foundation of Korea grant funded by the Korean Government (MEST) (20100027955).

## REFERENCES

1. Li Y, Gao GH, Lee DS. Stimulus-sensitive polymeric nanoparticles and their applications as drug and gene carriers. Adv Healthc Mater. 2013;2:388–417.
2. Toy R, Bauer L, Hoimes C, Ghaghada KB, Karathanasis E. Targeted nanotechnology for cancer imaging. Adv Drug Deliv Rev. 2014;76:79–97.
3. Li C. A targeted approach to cancer imaging and therapy. Nat Mater. 2014;13:110–5.
4. Schroeder A, Heller DA, Winslow MM, Dahlman JE, Pratt GW, Langer R, *et al.* Treating metastatic cancer with nanotechnology. Nat Rev Cancer. 2012;12:39–50.
5. Maeda H, Wu J, Sawa T, Matsumura Y, Hori K. Tumor vascular permeability and the EPR effect in macromolecular therapeutics: a review. J Control Release. 2000;65:271–84.
6. Maeda H, Nakamura H, Fang J. The EPR effect for macromolecular drug delivery to solid tumors: improvement of tumor uptake, lowering of systemic toxicity, and distinct tumor imaging *in vivo*. Adv Drug Deliv Rev. 2013;65:71–9.
7. Fang J, Nakamura H, Maeda H. The EPR effect: unique features of tumor blood vessels for drug delivery, factors involved, and limitations and augmentation of the effect. Adv Drug Deliv Rev. 2011;63:136–51.
8. Yin H, Liao L, Fang J. Enhanced permeability and retention (EPR) effect based tumor targeting: the concept, application and prospect. JSM Clin Oncol Res. 2014;2:1010.
9. Azzopardi EA, Ferguson EL, Thomas DW. The enhanced permeability retention effect: a new paradigm for drug targeting in infection. J Antimicrob Chemother. 2013;68:257–74.
10. Cheng Y, Morshed RA, Auffinger B, Tobias AL, Lesniak MS. Multifunctional nanoparticles for brain tumor imaging and therapy. Adv Drug Deliv Rev. 2014;66:42–57.
11. Torchilin V. Tumor delivery of macromolecular drugs based on the EPR effect. Adv Drug Deliv Rev. 2011;63:131–5.
12. Gao GH, Im GH, Kim MS, Lee JW, Yang J, Jeon H, *et al.* Magnetite-nanoparticle-encapsulated pH-responsive polymeric micelle as an MRI probe for detecting acidic pathologic areas. Small. 2010;6:1201–4.
13. Gao GH, Lee JW, Nguyen MK, Im GH, Yang J, Heo H, *et al.* pH-responsive polymeric micelle based on PEG-poly(beta-amino ester)/(amido amine) as intelligent vehicle for magnetic resonance imaging in detection of cerebral ischemic area. J Control Release. 2011;155:11–7.
14. Yang HY, Jang MS, Gao GH, Lee JH, Lee DS. pH-responsive biodegradable polymeric micelles with anchors to interface magnetic nanoparticles for MR imaging in detection of cerebral ischemic area. Nanoscale. 2016. doi:10.1039/C5NR06542A.
15. Wu XL, Kim JH, Koo H, Bae SM, Shin H, Kim MS, *et al.* Tumor-targeting peptide conjugated pH-responsive micelles as a potential drug carrier for cancer therapy. Bioconjugate Chem. 2010;21:208–13.
16. Zhou K, Wang Y, Huang X, Luby-Phelps K, Sumer BD, Gao J. Tunable, ultrasensitive pH-responsive nanoparticles targeting specific endocytic organelles in living cells. Angew Chem Int Ed. 2011;50:6109–14.
17. Wadajkar AS, Menon JU, Tsai YS, Gore C, Dobin T, Gandee L, *et al.* Prostate cancer-specific thermo-responsive polymer-coated iron oxide nanoparticles. Biomaterials. 2013;34:3618–25.
18. Wang H, Ke F, Mararenko A, Wei Z, Banerjee P, Zhou S. Responsive polymer-fluorescent carbon nanoparticle hybrid nanogels for optical temperature sensing, near-infrared light-responsive drug release, and tumor cell imaging. Nanoscale. 2014;6:7443–52.

19. Zhu H, Li Y, Qiu R, Shi L, Wu W, Zhou S. Responsive fluorescent $Bi_2O_3$@PVA hybrid nanogels for temperature-sensing, dual-modal imaging, and drug delivery. Biomaterials. 2012;33:3058–69.
20. Sowers MA, McCombs JR, Wang Y, Paletta JT, Morton SW, Dreaden EC, *et al.* Redox-responsive branched-bottlebrush polymers for *in vivo* MRI and fluorescence imaging. Nat Commun. 2014;5:5460.
21. Li Y, Qian Y, Liu T, Zhang G, Liu S. Light-triggered concomitant enhancement of magnetic resonance imaging contrast performance and drug release rate of functionalized amphiphilic diblock copolymer micelles. Biomacromolecules. 2012;13:3877–86.
22. Iessi E, Marino ML, Lozupone F, Fais S, Milito AD. Tumor acidity and malignancy: novel aspects in the design of antitumor therapy. Cancer Ther. 2008;6:55–66.
23. Wu Y, Zhang W, Li J, Zhang Y. Optical imaging of tumor microenvironment. Am J Nucl Med Mol Imaging. 2013;3:1–15.
24. Webb BA, Chimenti M, Jacobson MP, Barber DL. Dysregulated pH: a perfect storm for cancer progression. Nat Rev Cancer. 2011;11:671–7.
25. Ling D, Hackett MJ, Hyeon T. Cancer imaging: lighting up tumours. Nat Mater. 2014;13:122–4.
26. Trequesser QL, Seznec H, Delville MH. Functionalized nanomaterials: their use as contrast agents in bioimaging: mono- and multimodal approaches. Nanotechnol Rev. 2013;2:125–69.
27. Gao GH, Li Y, Lee DS. Environmental pH-sensitive polymeric micelles for cancer diagnosis and targeted therapy. J Control Release. 2013;169:180–4.
28. Ge Z, Liu S. Functional block copolymer assemblies responsive to tumor and intracellular microenvironments for site-specific drug delivery and enhanced imaging performance. Chem Soc Rev. 2013;42:7289–325.
29. Kato Y, Ozawa S, Miyamoto C, Maehata Y, Suzuki A, Maeda T, *et al.* Acidic extracellular microenvironment and cancer. Cancer Cell Int. 2013;13:89.
30. Tredan O, Galmarini CM, Patel K, Tannock IF. Drug resistance and the solid tumor microenvironment. J Natl Cancer Inst. 2007;99:1441–54.
31. Li Y, Gao GH, Lee DS. pH-sensitive polymeric micelles based on amphiphilic polypeptide as smart drug carriers. J Polym Sci Pol Chem. 2013;51:4175–82.
32. Chen D, Xia X, Gu H, Xu Q, Ge J, Li Y, *et al.* pH-responsive polymeric carrier encapsulated magnetic nanoparticles for cancer targeted imaging and delivery. J Mater Chem. 2011;21:12682–90.
33. Jin R, Lin B, Li D, Ai H. Superparamagnetic iron oxide nanoparticles for MR imaging and therapy: design considerations and clinical applications. Curr Opin Pharmacol. 2014;18:18–27.
34. Crayton SH, Tsourkas A. pH-titratable superparamagnetic iron oxide for improved nanoparticle accumulation in acidic tumor microenvironments. ACS Nano. 2011;5:9592–601.
35. Huang G, Chen H, Dong Y, Luo X, Yu H, Moore Z, *et al.* Superparamagnetic iron oxide nanoparticles: amplifying ROS stress to improve anticancer drug efficacy. Theranostics. 2013;3:116–26.
36. Zhu L, Wang D, Wei X, Zhu X, Li J, Tu C, *et al.* Multifunctional pH-sensitive superparamagnetic iron-oxide nanocomposites for targeted drug delivery and MR imaging. J Control Release. 2013;169:228–38.
37. Guo M, Yan Y, Liu X, Yan H, Liu K, Zhang H, *et al.* Multilayer nanoparticles with a magnetite core and a polycation inner shell as pH-responsive carriers for drug delivery. Nanoscale. 2010;2:434–41.
38. Ma WF, Wu KY, Tang J, Li D, Wei C, Guo J, *et al.* Magnetic drug carrier with a smart pH-responsive polymer network shell for controlled delivery of doxorubicin. J Mater Chem. 2012;22:15206–14.
39. Yang S, Chen D, Li N, Mei X, Qi X, Li H, *et al.* A facile preparation of targetable pH-sensitive polymeric nanocarriers with encapsulated magnetic nanoparticles for controlled drug release. J Mater Chem. 2012;22:25354–61.
40. Davies GL, Kramberger I, Davis JJ. Environmentally responsive MRI contrast agents. Chem Commun. 2013;49:9704–21.
41. Liu T, Li X, Qian Y, Hu X, Liu S. Multifunctional pH-disintegrable micellar nanoparticles of asymmetrically functionalized beta-cyclodextrin-based star copolymer covalently conjugated with doxorubicin and DOTA-Gd moieties. Biomaterials. 2012;33:2521–31.
42. Okada S, Mizukami S, Kikuchi K. Switchable MRI contrast agents based on morphological changes of pH-responsive polymers. Bioorg Med Chem. 2012;20:769–74.
43. Okada S, Mizukami S, Sakata T, Matsumura Y, Yoshioka Y, Kikuchi K. Ratiometric MRI sensors based on core-shell nanoparticles for quantitative pH imaging. Adv Mater. 2014;26:2989–92.
44. Huang X, Huang G, Zhang S, Sagiyama K, Togao O, Ma X, *et al.* Multi-chromatic pH-activatable $^{19}$F-MRI nanoprobes with binary ON/OFF pH transitions and chemical-shift barcodes. Angew Chem Int Edit. 2013;52:8074–8.
45. Wang K, Peng H, Thurecht KJ, Puttick S, Whittaker AK. pH-responsive star polymer nanoparticles: potential $^{19}$F MRI contrast agents for tumour-selective imaging. Polym Chem. 2013;4:4480–9.
46. Zhang S, Zhou K, Huang G, Takahashi M, Sherry AD, Gao J. A novel class of polymeric pH-responsive MRI CEST agents. Chem Commun. 2013;49:6418–20.
47. Battistelli G, Cantelli A, Guidetti G, Manzi J, Montalti M. Ultrabright and stimuli-responsive fluorescent nanoparticles for bioimaging. Wiley Interdiscip Rev Nanomed Nanobiotechnol. 2016;8:139–50.
48. Chinen AB, Guan CM, Ferrer JR, Barnaby SN, Merkel TJ, Mirkin CA. Nanoparticle probes for the detection of cancer biomarkers, cells, and tissues by fluorescence. Chem Rev. 2015;115:10530–74.
49. Li C, Liu S. Polymeric assemblies and nanoparticles with stimuli-responsive fluorescence emission characteristics. Chem Commun. 2012;48:3262–78.
50. Qiu F, Huang Y, Zhu X. Fluorescent unimolecular conjugated polymeric micelles for biological applications. Macromol Chem Physic. 2016;217:266–83.
51. Wolfbeis OS. An overview of nanoparticles commonly used in fluorescent bioimaging. Chem Soc Rev. 2015;44:4743–68.
52. Ko JY, Park S, Lee H, Koo H, Kim MS, Choi K, *et al.* pH-sensitive nanoflash for tumoral acidic pH imaging in live animals. Small. 2010;6:2539–44.
53. Wang Y, Zhou K, Huang G, Hensley C, Huang X, Ma X, *et al.* A nanoparticle-based strategy for the imaging of a broad range of tumours by nonlinear amplification of microenvironment signals. Nat Mater. 2014;13:204–12.
54. Wang W, Cheng D, Gong F, Miao X, Shuai X. Design of multifunctional micelle for tumor-targeted intracellular drug release and fluorescent imaging. Adv Mater. 2012;24:115–20.
55. Chan YH, Wu C, Ye F, Jin Y, Smith PB, Chiu DT. Development of ultrabright semiconducting polymer dots for ratiometric pH sensing. Anal Biochem. 2011;83:1448–55.
56. Urano Y, Asanuma D, Hama Y, Koyama Y, Barrett T, Kamiya M, *et al.* Selective molecular imaging of viable cancer cells with pH-activatable fluorescence probes. Nat Med. 2009;15:104–9.
57. Koo H, Lee H, Lee S, Min KH, Kim MS, Lee DS, *et al. In vivo* tumor diagnosis and photodynamic therapy via tumoral pH-

responsive polymeric micelles. Chem Commun. 2010;46:5668–70.
58. Zhou K, Liu H, Zhang S, Huang X, Wang Y, Huang G, *et al.* Multicolored pH-tunable and activatable fluorescence nanoplatform responsive to physiologic pH stimuli. J Am Chem Soc. 2012;134:7803–11.
59. Ma X, Wang Y, Zhao T, Li Y, Su LC, Wang Z, *et al.* Ultra-pH-sensitive nanoprobe library with broad pH tunability and fluorescence emissions. J Am Chem Soc. 2014;136:11085–92.
60. Duan Z, Gao YJ, Qiao ZY, Qiao S, Wang Y, Hou C, *et al.* pH-sensitive polymer assisted self-aggregation of bis(pyrene) in living cells in situ with turn-on fluorescence. Nanotechnology. 2015;26:355703.
61. Georgiev NI, Bryaskova R, Tzoneva R, Ugrinova I, Detrembleur C, Miloshev S, *et al.* A novel pH sensitive water soluble fluorescent nanomicellar sensor for potential biomedical applications. Bioorg Med Chem. 2013;21:6292–302.
62. Wang XD, Stolwijk JA, Lang T, Sperber M, Meier RJ, Wegener J, *et al.* Ultra-small, highly stable, and sensitive dual nanosensors for imaging intracellular oxygen and pH in cytosol. J Am Chem Soc. 2012;134:17011–4.
63. Ding D, Kwok RTK, Yuan Y, Feng G, Tang BZ, Liu B. A fluorescent light-up nanoparticle probe with aggregation-induced emission characteristics and tumor-acidity responsiveness for targeted imaging and selective suppression of cancer cells. Mater Horiz. 2015;2:100–5.
64. Fu L, Sun C, Yan L. Galactose targeted pH-responsive copolymer conjugated with near infrared fluorescence probe for imaging of intelligent drug delivery. ACS Appl Mater Interfaces. 2015;7:2104–15.
65. Biju V. Chemical modifications and bioconjugate reactions of nanomaterials for sensing, imaging, drug delivery and therapy. Chem Soc Rev. 2014;43:744–64.
66. Liand J, Zhu JJ. Quantum dots for fluorescent biosensing and bioimaging applications. Analyst. 2013;138:2506–15.
67. Probst CE, Zrazhevskiy P, Bagalkot V, Gao X. Quantum dots as a platform for nanoparticle drug delivery vehicle design. Adv Drug Deliv Rev. 2013;65:703–18.
68. Zhu H, Zhang S, Ling Y, Meng G, Yang Y, Zhang W. pH-responsive hybrid quantum dots for targeting hypoxic tumor siRNA delivery. J Control Release. 2015;220:529–44.
69. Li Z, Xu W, Wang Y, Shah BR, Zhang C, Chen Y, *et al.* Quantum dots loaded nanogels for low cytotoxicity, pH-sensitive fluorescence, cell imaging and drug delivery. Carbohydr Polym. 2015;121:477–85.
70. Pu KY, Liu B. Fluorescent conjugated polyelectrolytes for bioimaging. Adv Funct Mater. 2011;21:3408–23.
71. Wu C, Schneider T, Zeigler M, Yu J, Schiro PG, Burnham DR, *et al.* Bioconjugation of ultrabright semiconducting polymer dots for specific cellular targeting. J Am Chem Soc. 2010;132:15410–7.
72. Rong Y, Wu C, Yu J, Zhang X, Ye F, Zeigler M, *et al.* Multicolor fluorescent semiconducting polymer dots with narrow emissions and high brightness. ACS Nano. 2013;7:376–84.
73. Wu C, Chiu DT. Highly fluorescent semiconducting polymer dots for biology and medicine. Angew Chem Int Ed. 2013;52:3086–109.
74. Mohan P, Rapoport N. Doxorubicin as a molecular nanotheranostic agent: effect of doxorubicin encapsulation in micelles or nanoemulsions on the ultrasound-mediated intracellular delivery and nuclear trafficking. Mol Pharm. 2010;7:1959–73.
75. Bui QN, Li Y, Jang MS, Huynh DP, Lee JH, Lee DS. Redox- and pH-sensitive polymeric micelles based on poly(β-amino ester)-grafted disulfide methylene oxide poly(ethylene glycol) for anticancer drug delivery. Macromolecules. 2015;48:4046–54.
76. Guo X, Shi C, Wang J, Di S, Zhou S. pH-triggered intracellular release from actively targeting polymer micelles. Biomaterials. 2013;34:4544–54.
77. Prabaharan M, Grailer JJ, Pilla S, Steeber DA, Gong S. Amphiphilic multi-arm-block copolymer conjugated with doxorubicin via pH-sensitive hydrazone bond for tumor-targeted drug delivery. Biomaterials. 2009;30:5757–66.
78. Yang HY, Jang MS, Gao GH, Lee JH, Lee DS. Construction of redox/pH dual stimuli-responsive PEGylated polymeric micelles for intracellular doxorubicin delivery in liver cancer. Polym Chem. 2016;7:1813–25.
79. Zhu L, Tu C, Zhu B, Su Y, Pang Y, Yan D, *et al.* Construction and application of pH-triggered cleavable hyperbranched polyacylhydrazone for drug delivery. Polym Chem. 2011;2:1761–8.
80. Lee S, Chen X. Dual-modality probes for *in vivo* molecular imaging. Mol Imaging. 2009;8:87–100.
81. Ali Z, Abbasi AZ, Zhang F, Arosio P, Lascialfari A, Casula MF, *et al.* Multifunctional nanoparticles for dual imaging. Anal Chem. 2011;83:2877–82.
82. Jennings LE, Long NJ. 'Two is better than one'-probes for dual-modality molecular imaging. Chem Commun. 2009;24:3511–24.
83. Townsend DW. Dual-modality imaging: combining anatomy and function. J Nucl Med. 2008;49:938–55.
84. Gao G, Heo H, Lee J, Lee D. An acidic pH-triggered polymeric micelle for dual-modality MR and optical imaging. J Mater Chem. 2010;20:5454–61.
85. Ling D, Park W, Park SJ, Lu Y, Kim KS, Hackett MJ, *et al.* Multifunctional tumor pH-sensitive self-assembled nanoparticles for bimodal imaging and treatment of resistant heterogeneous tumors. J Am Chem Soc. 2014;136:5647–55.
86. Hu J, Liu T, Zhang G, Jin F, Liu S. Synergistically enhance magnetic resonance/fluorescence imaging performance of responsive polymeric nanoparticles under mildly acidic biological milieu. Macromol Rapid Commun. 2013;34:749–58.
87. Kim KS, Park W, Hu J, Bae YH, Na K. A cancer-recognizable MRI contrast agents using pH-responsive polymeric micelle. Biomaterials. 2014;35:337–43.
88. Wang C, Cheng L, Liu Y, Wang X, Ma X, Deng Z, *et al.* Imaging-guided pH-sensitive photodynamic therapy using charge reversible upconversion nanoparticles under near-infrared light. Adv Funct Mater. 2013;23:3077–86.
89. Cheng R, Meng F, Deng C, Klok HA, Zhong Z. Dual and multi-stimuli responsive polymeric nanoparticles for programmed site-specific drug delivery. Biomaterials. 2013;34:3647–57.
90. Onaca O, Enea R, Hughes DW, Meier W. Stimuli-responsive polymersomes as nanocarriers for drug and gene delivery. Macromol Biosci. 2009;9:129–39.
91. Schmaljohann D. Thermo- and pH-responsive polymers in drug delivery. Adv Drug Deliv Rev. 2006;58:1655–70.
92. Torchilin VP. Multifunctional, stimuli-sensitive nanoparticulate systems for drug delivery. Nat Rev Drug Discov. 2014;13:813–27.
93. Sundaresan V, Menon JU, Rahimi M, Nguyen KT, Wadajkar AS. Dual-responsive polymer-coated iron oxide nanoparticles for drug delivery and imaging applications. Int J Pharm. 2014;466:1–7.
94. Bhattacharya D, Behera B, Sahu SK, Ananthakrishnan R, Maiti TK, Pramanik P. Design of dual stimuli responsive polymer modified magnetic nanoparticles for targeted anti-cancer drug delivery and enhanced MR imaging. New J Chem. 2016;40:545–57.
95. Yin L, He C, Huang C, Zhu W, Wang X, Xu Y, *et al.* A dual pH and temperature responsive polymeric fluorescent sensor and its imaging application in living cells. Chem Commun. 2012;48:4486–8.

96. Liu Y, Li C, Wang HY, Zhang XZ, Zhuo RX. Synthesis of thermo- and pH-sensitive polyion complex micelles for fluorescent imaging. Chem Eur J. 2012;18:2297–304.
97. Wu W, Aiello M, Zhou T, Berliner A, Banerjee P, Zhou S. In-situ immobilization of quantum dots in polysaccharide-based nanogels for integration of optical pH-sensing, tumor cell imaging, and drug delivery. Biomaterials. 2010;31: 3023–31.
98. Wu W, Shen J, Banerjee P, Zhou S. Chitosan-based responsive hybrid nanogels for integration of optical pH-sensing, tumor cell imaging and controlled drug delivery. Biomaterials. 2010;31: 8371–81.
99. Wu W, Zhou T, Berliner A, Banerjee P, Zhou S. Smart core-shell hybrid nanogels with Ag nanoparticle core for cancer cell imaging and gel shell for pH-regulated drug delivery. Chem Mater. 2010;22:1966–76.
100. Jiang L, Zhou Q, Mu K, Xie H, Zhu Y, Zhu W, *et al.* pH/temperature sensitive magnetic nanogels conjugated with Cy5.5-labled lactoferrin for MR and fluorescence imaging of glioma in rats. Biomaterials. 2013;34:7418–28.
101. Sahoo B, Devi KS, Banerjee R, Maiti TK, Pramanik P, Dhara D. Thermal and pH responsive polymer-tethered multifunctional magnetic nanoparticles for targeted delivery of anticancer drug. ACS Appl Mater Interfaces. 2013;5:3884–93.